

# Lawrence Berkeley National Laboratory

## Recent Work

### Title

GAMMA and ALPHA DECAY FROM THE 2.1-msec ISOMER  $^{213}\text{mRa}$

### Permalink

<https://escholarship.org/uc/item/6vb6p0pv>

### Author

Raich, D.G.

### Publication Date

1976-07-01

0 0 0 0 4 5 0 4 6 4 5

Submitted to Zeitschrift fuer Physik

LBL-5049  
Preprint **21**

GAMMA AND ALPHA DECAY FROM THE  
2.1-msec ISOMER  $^{213}\text{mRa}$

D. G. Raich, H. R. Bowman, R. E. Eppley,  
J. O. Rasmussen, and I. Rezanka

RECEIVED  
GENERAL  
LABORATORY  
AUG 12 1976

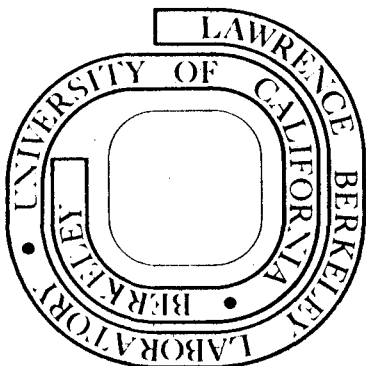
July 1976

LIBRARY AND  
DOCUMENTS SECTION

Prepared for the U. S. Energy Research and  
Development Administration under Contract W-7405-ENG-48

**For Reference**

Not to be taken from this room



LBL-5049  
**21**

## **DISCLAIMER**

This document was prepared as an account of work sponsored by the United States Government. While this document is believed to contain correct information, neither the United States Government nor any agency thereof, nor the Regents of the University of California, nor any of their employees, makes any warranty, express or implied, or assumes any legal responsibility for the accuracy, completeness, or usefulness of any information, apparatus, product, or process disclosed, or represents that its use would not infringe privately owned rights. Reference herein to any specific commercial product, process, or service by its trade name, trademark, manufacturer, or otherwise, does not necessarily constitute or imply its endorsement, recommendation, or favoring by the United States Government or any agency thereof, or the Regents of the University of California. The views and opinions of authors expressed herein do not necessarily state or reflect those of the United States Government or any agency thereof or the Regents of the University of California.

Gamma and Alpha Decay from the 2.1-msec Isomer  $^{213\text{m}}\text{Ra}$ D. G. Raich<sup>\*</sup>, H. R. Bowman, R. E. Eppley<sup>+</sup>, J. O. Rasmussen

Lawrence Berkeley Laboratory, University of California, Berkeley CA 94720

and

I. Rezanka<sup>‡</sup>

Heavy Ion Accelerator Laboratory, Yale University, New Haven, CT 06520

---

<sup>\*</sup>Present address: Chemistry Division, Argonne National Laboratory,  
Argonne, IL 60439

<sup>+</sup>Present address: Monsanto Research Corp., Mound Laboratory,  
Miamisburg, OH 45342

<sup>‡</sup>Present address: Research Laboratory, Xerox Corp.,  
Rochester, New York 14600

---

Abstract: The isomer  $^{213m}\text{Ra}$  was produced by the reaction  $^{209}\text{Bi}(^{10}\text{B}, 6n)$ , as well as by bombardments of  $^{12}\text{C}$  on Pb isotopes,  $^{14}\text{N}$  on Bi, and  $^{16}\text{O}$  on natural Hg, with projectile energies in the range 60-100 MeV. The isomer decays with a half-life of 2.1 ms both via gamma internal transitions and via alpha branching to levels in  $^{209}\text{Rn}$ . A level scheme is proposed in which the isomeric state is assigned as either  $17/2^-$  or  $13/2^+$  with shell-model configurations either of the  $h_{9/2}$  protons coupled to a  $p_{1/2}$  neutron hole, or of an uncoupled  $i_{13/2}$  neutron hole. On the basis of alpha decay rate predictions from the new Fliessbach theory, the  $17/2^-$  isomeric assignment is to be preferred.

Phys. Abstracts classifications 4.200-4.375

E [RADIOACTIVITY  $^{213m}\text{Ra}$  [from  $^{209}\text{Bi}(^{10}\text{B}, 6n)$ ,  $^{204-6}\text{Pb}(^{12}\text{C}, 3n-5n)$  etc.,  $E = 60-100$  MeV]; measured  $E_\alpha$ ,  $E_\gamma$ ,  $I_\alpha$ ,  $I_\gamma$ ,  $I_x$ ,  $\gamma\gamma$ -coin,  $x\gamma$ -coin,  $\alpha K$ ,  $T_{1/2}$ .  $^{213}\text{Ra}$ ,  $^{209}\text{Rn}$  deduced levels,  $J$ ,  $\pi$ ,  $\gamma$ -multipolarity.]

## 1. Introduction

With the advent of computer-based data collection systems, the 10-Hz 2% duty cycle of Yale University's Heavy Ion Accelerator (HILAC) was found to be particularly well suited to the investigation of activities with halflives in the millisecond range. Such activities would be visible at the end of each 2-ms beam burst, but would decay completely during the 100 ms between bursts. Prior to the shutdown of Yale HILAC, the Nuclear Chemistry group there engaged in a series of investigations of such short-lived activities in the neutron-deficient nuclides characteristically produced by heavy-ion reactions. The work described here began with a survey for new millisecond activities near the "island of isomerism" that is found before the shell closure of the 126-neutron isotones. Gamma-ray spectroscopy of  $^{213\text{m}}\text{Ra}$ , a millisecond isomer thus discovered, was completed at Yale. After the shutdown of that facility, when it was realized that the isomer decayed via an alpha branch as well, the experiments continued with alpha-particle spectroscopy at the Berkeley SuperHILAC.

## 2. Experimental Configuration

### 2.1 Gamma spectroscopy

In most of the experimental runs a heavy-metal target foil was placed at about a  $45^\circ$  angle in the Yale HILAC beam. Counting was carried out simultaneously with irradiation, using a detector positioned  $90^\circ$  from the beam line, obliquely facing the front of the target. Adequate statistics could be accumulated this way in a few hours of running.

The beams were of such nuclei as  $^{10}\text{B}$ ,  $^{12}\text{C}$ ,  $^{14}\text{N}$ , and  $^{16}\text{O}$  at laboratory energies between 5 and 10 MeV/nucleon. The intensity was usually kept fairly low (on the order of nano-amperes) to avoid swamping the detector during beam bursts. In the earlier survey and cross-bombardment runs, fairly thick ( $>50\text{ mg/cm}^2$ ) targets of natural Au, Hg, Pb, and Bi were used; later we concentrated on thin ( $5\text{-}10\text{ mg/cm}^2$ ) self-supporting foils of bismuth produced by cold rolling or vacuum deposition. Bismuth was a convenient target material for the more detailed investigations of  $^{213}\text{Ra}$  since it is naturally monoisotopic, thus giving a cleaner reaction. We employed several high-resolution Ge(Li) detectors with volumes around  $10\text{-}40\text{ cm}^3$  placed about 5 cm from the target, outside the vacuum, and separated from the target by a plexiglas, mylar, or thin aluminum window. In some runs we used a  $500\text{-mm}^3$  intrinsic Ge detector for better resolution of x-rays and low-energy  $\gamma$ -rays. Spectra were accumulated by a PDP-8/I computer system. Several data collection programs were used, but in general the process involved starting the counting at the end of each beam burst and switching the counting from one storage block to another at preset intervals during the 100 ms between bursts. Thus, a series of spectra could be accumulated, each showing the activity during a particular several-millisecond interval following irradiation. The data were analyzed both by hand from computer-generated plots of the spectra and by various programs, including versions of the Lawrence Berkeley Laboratory's SAMPO[1], on PDP-10, IBM 7094 DCS, and CDC 7600 computer systems.

For the coincidence experiments, a second Ge(Li) detector was placed  $180^\circ$  from the first, obliquely facing the back of the thin target. Three- and four-parameter coincidence events ( $E_1$ ,  $E_2$ , nanosecond time between the two  $\gamma$ -rays, and sometimes millisecond time since beam burst) were recorded serially on magnetic tape by the PDP-8/I for later computer sorting and analysis.

Also, to help in identifying the millisecond activities, a stacked-foil excitation-function run was made to trace the decay chains. For this we constructed a stack of six  $\approx 3 \text{ mg/cm}^2$  Al foils on which  $\approx 2 \text{ mg/cm}^2$  of Bi had been evaporated. The aluminum foils served both as supports and as beam degraders so that the bismuth layers were exposed to beam energies between 60 and 90 MeV. The stack was irradiated with a 105-MeV beam of  $^{10}\text{B}$  at  $\approx 1$  particle- $\mu\text{A}$  for about 6 hours, and the individual foils were then counted several times during the following week with a high-resolution Ge(Li)  $\gamma$ -spectrometer. The spectra were analyzed as described earlier. Since the activity induced in the aluminum support foils decayed in a matter of hours, no chemical separation was required. Thus, reaction product decay chains could easily be followed by observing the  $\gamma$ -activity due to EC-decay of their members.



## 2.2 Alpha spectroscopy

The alpha spectroscopy experiments were performed at Berkeley SuperHILAC using the helium-jet technique to catch recoiling reaction products and transfer them to a low-background counting chamber. Our apparatus is illustrated in Fig. 1. It was designed and built by E. K. Hyde and co-workers, and is described more fully in [2,3].

We used a  $^{12}\text{C}$  beam at the full 7.2-MeV/amu energy of SuperHILAC (86.4 MeV), but the degrader foils and protective windows reduced this to the range 55-70 MeV. The targets were of lead isotopes, including one enriched in  $^{206}\text{Pb}$  (97.22% of 206, 1.34% of 207, 1.39% of 208), and one enriched in  $^{204}\text{Pb}$  (73.3% of 204, 12.03% of 206, 5.90% of 207, 8.77% of 208); the material was assayed by the supplier, Oak Ridge National Laboratory. The experiments using the  $^{204}\text{Pb}$  target were the most successful; it consisted of a  $600\ \mu\text{g}/\text{cm}^2$  film evaporated onto the back of a nickel support foil that also served as the He-cell window (thus reducing beam degradation). We were not able to use the combination of a  $^{10}\text{B}$  beam and  $^{209}\text{Bi}$  target that had proved so successful in the gamma spectroscopy experiments, because the required 8-MeV/amu beam energy (80 MeV) was beyond the capabilities of SuperHILAC after its mass range had been extended.

Product recoils were thermalized in 2 atm of helium and jetted through an 0.18-mm-i.d. capillary to a collector plate facing an annular Si(Au) surface-barrier particle detector.

The spectrum collection philosophy was much the same as described above for gamma spectroscopy; alpha spectra were accumulated in a series of short time intervals between beam bursts.

We used the smallest available He-cell volume ( $5\text{-cm}^3$ ), and measured a flow rate of  $27\text{ cm}^3/\text{sec}$ , for an average turnover time of 180 ms. Since the SuperHILAC beam was pulsed every 27.8 ms, one would expect only a 15% turnover of the cell volume between beam bursts. However, we observed that 25% of the recoils produced in each beam burst actually were delivered much more rapidly -- with an approximately Gaussian differential delivery function having 1.9-ms standard deviation halfwidth, and a mean delivery time of 8.2 ms. We performed this calibration by observing the time distribution of the 1.7-ms  $\alpha$ -particles of  $^{215}\text{Ra}$  (cf. Fig. 2). The observed distribution can be fit fairly well assuming a Gaussian differential delivery function folded into the known half-life, and we thus obtain  $N_0$  as a fitting parameter. (Actually, it can be seen that the delivery function rises a little more rapidly and drops off a little more slowly than a Gaussian, a behavior qualitatively similar to that observed by Macfarlane[4]. However, the Gaussian has the advantage of being expressible in closed form and seems adequate for the  $N_0$  calculation.) In addition, we measured the steady-state decay rate of  $^{213}\text{Ra}$ . Taking alpha branching ratios into account, we calculated the apparent production ratio between  $^{213}\text{Ra}$  and  $^{215}\text{Ra}$ . Assuming that the two

radium isotopes are produced with equal cross-sections in the ( $^{12}\text{C}, 3n$ ) reactions on  $^{204}\text{Pb}$  and  $^{206}\text{Pb}$ , we expect the actual production ratio to be equal to the ratio of the 204 and 206 isotopes in the lead target. The rapidly delivered fraction of  $^{215}\text{Ra}$  accounts for 25% of the expected production. Evidently, the helium flow through the cell was far from uniform. Probably a small central volume of the cell was exchanged very rapidly by a vortex extending directly across from the inlet to the capillary. The remainder of the cell volume was exchanged less rapidly.

### 3. Experimental Results

The characteristic gamma spectrum of  $^{213\text{m}}\text{Ra}$ , consisting of three prominent lines at 160.87, 546.35, and 1062.5 keV decaying with a half-life of  $2.1 \pm 0.1$  ms (see Fig. 3), was first observed in a survey run wherein a thick natural  $^{80}\text{Hg}$  target was bombarded with  $^{16}_8\text{O}$  at several energies in the region of 100 MeV. At these energies the resulting  $^{212-220}_{88}\text{Ra}^*$  compound-nuclei could be expected either to fission or to boil off as many as eight neutrons and/or several charged particles before reaching the 2.1-ms state. However, in the same experiment two other targets, of natural  $^{82}\text{Pb}$  and  $^{79}\text{Au}$ , were bombarded without producing the millisecond activity. Hence it probably was not due to a fission product.

Attempting to identify the millisecond gamma emitter, we performed several additional bombardments on thick natural

targets at comparable projectile energies. The most significant of these targets were  $^{209}_{83}\text{Bi} + ^{10}_5\text{B}$ ,  $^{209}_{83}\text{Bi} + ^{14}_7\text{N}$ , and  $^{204-208}_{82}\text{Pb} + ^{10}_5\text{B}$ . The characteristic millisecond activity was observed in all but the last of these bombardments. Thus it was concluded that the activity was due either to decay of a radium isotope or to internal transitions from an isomeric state within radium. Hence, the applicable reaction mechanism in the  $\text{Hg} + ^{16}_8\text{O}$  and  $\text{Bi} + ^{10}_5\text{B}$  systems would be strictly (HI,xn).

In subsequent experiments we concentrated for the most part on the reaction of  $^{209}\text{Bi} + ^{10}\text{B}$  in thin targets, taking advantage of natural bismuth's having a single isotope. Our use of the rarer boron isotope posed no problems since the Yale HILAC was capable of producing beams several orders of magnitude more intense than we could use when counting during and between beam bursts.

We found that the excitation function for production of the millisecond activity by this reaction is sharply peaked near 80-MeV lab projectile energies (see Fig. 4, top). The sharply peaked shape is characteristic of (HI,xn) compound-nucleus reactions. Moreover, the 80-MeV peak allowed us to conclude that the reaction was most likely  $^{209}\text{Bi}(^{10}\text{B},6n)^{213}\text{Ra}$ . On the basis of interpolation to the  $^{219}\text{Ra}^*$  compound nucleus from previously reported reactions via  $^{218}\text{Ra}^*$  and  $^{220}\text{Ra}^*$  intermediates [5,6], we could estimate that the 6n reaction should peak near 78 MeV, while the 5n and 7n reactions should predominate roughly 13 MeV lower and higher, respectively.

The stacked-foil experiment confirmed this mass assignment. The excitation function of the  $^{213}\text{Ra}$  granddaughter,  $^{209}\text{At}$  (obtained by observing the gamma activity of its 5.4-h EC-decay to  $^{209}\text{Po}$ ), is similar to that of the millisecond activity. As shown in the lower half of Fig. 4, members of all four decay chains were examined. None of the others contained comparable excitation functions; thus, the millisecond activity clearly is due to a mass  $4n+1$  nucleus. Since all nuclei in the decay chains connecting  $^{213}\text{Ra}$  ( $T_{1/2} = 2.74$  min) and  $^{209}\text{Po}$  have half-lives that are on the order of seconds or minutes, it is evident that the 2.1-ms activity must result from an isomeric state in  $^{213}\text{Ra}$ .

In more detailed investigations, we measured the halflife of the millisecond activity and obtained accurate photon energies and intensities. These results are summarized in Table 1. The  $\gamma$ -rays reported in the lower portion of Table 1 as being due to  $^{209}\text{Rn}$  internal transitions are part of the evidence that led us to suspect direct  $\alpha$ -branching from the isomer. They are seen clearly only in the high-resolution x-ray spectra. Perversely, as can be seen in Fig. 3, the most intense of these at 214.7 keV also suffers interference from a more intense 210.45-keV  $\gamma$ -ray that we now assign to the fission products  $^{103\text{m}}\text{Ru}$  in millisecond spectra and  $^{103}\text{Tc}$  in spectra taken over a time scale of minutes.

We found, in the coincidence experiments, that the three prominent lines are coincident with one another and with the Ra K x-rays, in a cascade that occurs faster than our 10-ns time resolution. The other three lines were too weak to be considered seriously in the coincidence sorts, but the stronger two (110.1 and 214.7 keV) do seem to be absent. These results are summarized in Table 3. The coincidences with radium x-rays are a final confirmation of our assignment of the isomer. More important, however, is the fact that from the coincident x-ray intensities, we can calculate K-conversion coefficients ( $\alpha_K$ ) for the transitions and thus make the tentative multipolarity assignments, as shown in the last column of Table 3.

We had developed a tentative level scheme, not too different from that finally adopted, by the time we decided to look via He-jet  $\alpha$ -spectroscopy for direct evidence of the isomer's alpha branching. To begin the search for such alpha activity, we first estimated the minimum possible energy of the isomeric state as 1769 keV, the sum of the three cascade transition energies (top of Table 1). The Q-value for ground-state  $^{213}\text{Ra}$   $\alpha$ -decay is 6.893 MeV (Table 4), so the minimum  $Q_\alpha$  for the isomer would be 8.662 MeV, which translates to an  $\alpha$ -particle energy of 8.47 MeV. Depending on which states were actually populated by the decay, this would probably be the highest member of a triplet, the other lines being 110 and 215 keV lower, corresponding to the first two excited states of  $^{209}\text{Rn}$  as reported by Valli and Hyde[3].

When we used the  $^{206}\text{Pb}$ -enriched target, we encountered strong interference from the twin doublets of the  $^{214}\text{Fr}$  and  $^{214}\text{Fr}^m$   $\alpha$ -groups. The francium energies are shown at the bottom of Table 4. They are ideally positioned to mask our expected  $^{213}\text{Ra}^m$  energies, especially since they also have millisecond halflives of 5.5 and 3.6 ms, respectively, for  $^{214}\text{Fr}$  and its isomer. The  $^{214}\text{Fr}$  is presumably produced both by reaction with the small  $^{207}\text{Pb}$  fraction in the target -- via the direct p4n-out reaction which should occur at nearly the same energy as  $^{206}\text{Pb}(^{12}\text{C},5n)^{213}\text{Ra}$  -- and via the direct p3n-out reaction with  $^{206}\text{Pb}$ . Moreover, we had to run with projectile energies of less than the 84-MeV optimum for the 5n-out reaction, under which conditions the latter reaction is increasingly favored. ( $^{214}\text{Rn}$  is not produced here in appreciable amounts by  $^{214}\text{Ra}$  EC-decay[5].)

We were able to reduce the  $^{214}\text{Fr}$  interference considerably by using a  $^{204}\text{Pb}$ -enriched target. The reaction  $^{204}\text{Pb}(^{12}\text{C},3n)^{213}\text{Ra}$  was expected to peak at about 61 MeV, very near the Coulomb barrier. Thus, the maximum cross section might be less than with the  $^{206}\text{Pb}$  target, but the low energy largely eliminates the competing  $^{214}\text{Fr}$  production, since the pn-out reaction cross-section should be greatly reduced. Moreover, while our  $^{204}\text{Pb}$  has a 12%  $^{206}\text{Pb}$  fraction (thus we see  $^{215}\text{Ra}$  for calibration), it has none of the non-naturally-occurring  $^{205}\text{Pb}$  isotope.

The total alpha spectrum (not time-sorted) from our runs at 63-68 MeV is shown in Fig. 5, and a detail at the energies of interest in two time intervals appears in Fig. 6. The line at 8.467 MeV decays more rapidly than the  $^{214}\text{Fr}$  lines we had seen before. It seems a likely candidate for assignment to  $^{213\text{m}}\text{Ra}$  inasmuch as it occurs at the anticipated minimum energy; and it cannot be due entirely to  $^{214\text{m}}\text{Fr}$  because the other equally intense member of that doublet at 8.546 MeV appears much weaker. About 110 keV lower we find another candidate for  $^{213\text{m}}\text{Ra}$   $\alpha$ -decay at 8.358 MeV and justify our assignment in a similar manner. Although 8.358 MeV is the energy of a  $^{214}\text{Fr}$  group, that group is known to be twenty times weaker than the 8.420-MeV  $^{214}\text{Fr}$  group; the line we see is about five times more intense than can be accounted for by  $^{214}\text{Fr}$ . Finally, 0.2 MeV below the first line, we see another very weak decaying line which might, on energetic grounds, be assigned to  $^{213\text{m}}\text{Ra}$ . Our spectroscopic measurements are summarized in Table 4.

#### 4. The Level Scheme

We propose the level scheme illustrated in Fig. 7 for states populated in the 2.1-ms  $^{213\text{m}}\text{Ra}$  decay. The  $^{213}\text{Ra}$  nucleus is sufficiently close to doubly-magic  $^{208}\text{Pb}$  that the spherical single-particle model should predict lower energy levels fairly well. We expect the single hole in the 126-neutron shell to dominate the configurations of the first few states, resulting in a ground state with  $J^\pi = 1/2^-$ , and first two excited states  $5/2^-$  and  $3/2^-$  (with the neutron hole successively occupying  $p_{1/2}$ ,



$f_{5/2}$ , and  $p_{3/2}$  shell-model orbitals). Higher-seniority configurations involving the  $h_{9/2}$  protons are expected to become significant somewhat above 1 MeV (see Table 5), and excitations of the  $^{208}\text{Pb}$  core should appear near 2.5 MeV. The systematics of pertinent levels in 125-neutron isotones may be followed in Fig. 8.

On the basis of trends in Fig. 8, a  $5/2^-$  state is expected in  $^{213}\text{Ra}$  near 540 keV. This seems the most likely origin for our 546.35-keV  $\gamma$ -ray. The transition consequently should be of E2 multipolarity. We could not measure the conversion coefficient  $\alpha_K$  very accurately for this  $\gamma$ -ray, but the value we obtain (Table 3) is seen from Table 2 to fit an E2 transition much better than any other multipolarity assignment.

The next level expected would be a  $3/2^-$  state in the vicinity of 830 keV. It would probably decay directly to ground more readily than to the  $5/2^-$  state, but we are unable to observe any  $\gamma$ -rays likely to have originated from that level in either case. It seems more likely that the  $3/2^-$  state is skipped in the isomeric gamma cascade, as is the case in the primary cascades of the other 125-neutron isotones. There is no other level in this region that might reasonably be the origin of the 160.87-keV transition, and we instead suppose that the  $5/2^-$ -level is fed entirely through the 1062.5-keV transition.

The resultant 1608.9-keV level is in the energy region of the  $\{\pi(h_{9/2}^6)_{J_p \neq 0} \nu p_{1/2}^{-1}\}_J$  multiplet; and on the basis of trends in Fig. 8, the most likely assignment is  $J^\pi = 9/2^-$  ( $J_p = 4$ ). This is also the most consistent interpretation from our intensity data. In Table 3 we can set the limit that  $\alpha_K < 0.015$ , but this is more consistent with electric- than magnetic-multipole transitions according to Table 2. Odd electric multipoles would connect the  $5/2^-$  state with an even-parity state; and since only odd-parity states are expected in the vicinity of 1600 keV, the transition is indicated to be E2 and the initial state would likely be  $9/2^-$ . From the gamma intensities we can use the appropriate theoretical total conversion coefficients in Table 2 to calculate the transition intensities. This has been done in the next-to-last column of Table 1 under the assumption of E2 transitions, where we find that the transition intensities thus calculated for the bottom members of the cascade, while not quite identical, are almost within experimental error. We know, however, that the  $9/2^-$  state's wave-function should have, in addition to the dominant  $\{\pi(h_{9/2}^6)_{J_p \neq 0} \nu p_{1/2}^{-1}\}$  configuration, admixtures involving  $f_{7/2}$  protons and also an  $h_{9/2}$  neutron hole[17].

Adding the 160.87-keV transition to the top of the cascade establishes a level at 1769.7 keV, which seems to be identical to the 1770-keV isomeric level deduced from measured  $\alpha$ -decay Q-values (Table 4). On the basis of x-ray coincidences,

$\alpha_K = 0.25$  for this transition, indicating that it is E2. Furthermore, when (in Table 1) K-vacancies are calculated using the E2 value of  $\alpha_K$ , this transition accounts for the bulk of the K-vacancies and the total is in excellent agreement with the observed K-x-ray transition intensity. The E2 value of  $\alpha_{\text{total}}$  balances the relative intensity of the 160.87-keV transition with the others. This would suggest that the 1769.7-keV state is  $13/2^-$ , again presumably in the  $\pi h_{9/2}^6$  multiplet. However, inasmuch as there can be a wide range of M1/E2 mixing ratios, we must consider the possibility that the state is  $11/2^-$  (also in the multiplet) and the 160.87-keV transition, has  $\Delta J = -1$  but is nearly 100% E2. In fact, a similarly placed 195-keV transition between  $11/2^-$  and  $9/2^-$  states in  $^{209}\text{Po}$  is M1 + ~20% E2[14].

If the 2.1-ms isomeric state is at 1769.7 keV and is depopulated by the 160.87-keV transition, the transition would most likely be enhanced E3 or M3 according to the Weisskopf single-particle lifetime estimate[17]. Certainly it would have to be severely hindered to be E2 or M1. Such a hindrance is highly unlikely between states of the multiplet, whether we assign the 1769.7-keV level as  $11/2^-$  or  $13/2^-$ . Therefore we set aside for a moment the question of  $J^\pi$  for this level, which apparently is not the isomeric state, given the E2-nature of the transition from it. Another assignment must be sought for the isomer.

Low-lying, high-spin states are a common cause of isomerism and are readily populated in heavy-ion reactions. Two candidates for such a state suggest themselves. First, on the basis of level trends we expect an  $i_{13/2}^{-1}$  ( $13/2^+$ ) neutron-hole state near 1800 keV. And second, in  $^{214}\text{Ra}$  the  $8^+ \pi(h_{9/2}^6)_8$  state at 1864 keV is isomeric, with an E2-transition half-life much longer than that seen for other E2's in similar cascades (see Table 5), probably reflecting cancellation in the pairing factor  $(U_i U_f - V_i V_f)^2$  near the half-filled  $h_{9/2}$  proton shell[18]. This  $\pi(h_{9/2}^6)_8$  state might couple in  $^{213}\text{Ra}$  with the  $p_{1/2}^{-1}$  neutron hole to produce a long-lived  $17/2^-$  state of about the correct energy. In a forthcoming paper[19] we test these two possibilities with Fliessbach's new normalized  $\alpha$ -decay theory[20] by comparing predictions of branching ratios to the daughter states from each of the hypothetical parent states. The pattern of intensities fits our  $\alpha$ -spectroscopic data much better assuming a  $17/2^-$  isomeric state, so we report this as our preferred interpretation.

The  $\alpha$ -decay measurements place the isomeric state at  $1770 \pm$  keV, very nearly the same energy as the state at the top of the gamma cascade. The isomeric transition is presumably an unobserved, highly-converted  $\gamma$ -transition of only a few keV, with energy below the K and L edges. The transition is a highly hindered E2 and the 1769.7-keV level is  $13/2^-$  if the isomer is  $17/2^-$ . The E2 possibility is tenable in light of

the retarded-E2 situation in the  $8^+$  state of  $^{214}\text{Ra}$  (retardation factor  $10^4$ ). (Assigning the 1769.7-keV level as  $11/2^-$  would require that the isomeric transition be M3 enhanced by a factor of  $10^3$ . Such a large enhancement is out of the question for an M3 transition.)

The characteristics of ground-state  $^{213}\text{Ra}$  decay were measured by Valli et al.[5] whose values, included in Fig. 7, are in agreement with our own (Table 4). The  $I^\pi$  level assignments for  $^{209}\text{Rn}$  are based on the systematics for 123-neutron isotones<sup>3)</sup>, with energies refined as a result of our gamma spectroscopy. The  $I^\pi$  assignments suggest that the 110.1-keV  $\gamma$ -transition is E2 and the other two are M1 or M1 + E2.

However, because of the weakness of the  $\gamma$ -rays in  $^{209}\text{Rn}$  with  $^{213}\text{Ra}$   $\alpha$ -decay, we have not been able reliably to confirm these assignments. In fact, there seems to be some inconsistency in our  $\gamma$ -ray intensity data. Certainly one would expect the ratio of the intensities of the two  $\gamma$ -rays depopulating the 214.7-keV level,  $I_\gamma(104.6)/I_\gamma(214.7)$ , to be the same for both millisecond and minute feeding, but it is three times larger in our minute-scale decay data. Of course, the very large error (>80%) in the millisecond-scale intensity of the 104.6-keV line may account for this discrepancy. A more serious criticism of the millisecond components of the intensities arises when we compare the feeding ratios derivable from alpha and gamma data. We know that the 2.74-min, ground-state  $^{213}\text{Ra}$

$\alpha$ -decay feeds the 110.1-keV level in  $^{209}\text{Rn}$  eight times more strongly than the 214.7-keV level. This feeding ratio is supported by the 2.74-min components of our gamma intensities (lowest section of Table 1), assuming mixed M1 + E2 transitions with probably dominant E2 character. Our alpha spectroscopy shows that 2.1-ms  $^{213\text{m}}\text{Ra}$  favors the 110.1-keV level similarly, feeding it at least nine times more strongly than the 214.7 keV level. However, the millisecond gamma intensities (middle section of Table 1) require nearly equal feedings to the two levels. Perhaps our millisecond intensities are being confused by interfering radiation. The apparent alpha branching ratio from the isomer on the basis of these gamma intensities is found to be  $\approx 7\%$ , which also appears to be high.

We obtain a more reliable isomeric branching ratio from the alpha spectroscopic data. As noted below Table 4, in the rapidly delivered He-jet fraction only 0.088% of the  $^{213}\text{Ra}$   $\alpha$ -decay comes from the isomer. The actual decay ratio should be roughly four times larger because only about a quarter of the production is swept out immediately from the reaction chamber during the first several milliseconds, while the longer-lived products will be in a steady-state equilibrium. In our gamma spectroscopy from the ratio of the isomer's intensity to that of the longer-lived daughters, such as  $^{209}\text{Rn}$  and  $^{209}\text{At}$ , we were able to deduce that at least 70% of the  $^{213}\text{Ra}$  is produced in the isomeric state by the heavy-ion reactions. Using the 80%

ground-state alpha-branching ratio measured by Valli et al.[5], we calculate that the alpha branching ratio of the isomer is at most 0.6%. We feel this value is considerably more reliable than the 7% value calculated above from gamma data, and thus the  $\approx 1\%$  figure that we show in Fig. 7 is heavily biased toward the alpha-spectroscopic determination.

---

### Acknowledgements

The authors wish to extend their sincere appreciation to the staffs of the Yale and Berkeley HILACs, who helped greatly in facilitating the experimental work. Particular thanks are due Mr. Solly Simone, formerly of Yale HILAC, for his practical suggestions on producing thin self-supporting targets by vacuum deposition. We also gratefully acknowledge helpful discussions with Dr. L. J. Jardine of the Lawrence Berkeley Laboratory. This work was supported by the U.S.-A.E.C. and E.R.D.A., and by a fellowship to one of the authors (J.O.R.) from the J. S. Guggenheim Foundation (1973).



References

1. J. R. Routti and S. G. Prussin: Nucl. Instr. Meth. 72, 125 (1969)
2. J. Borggreen, K. Valli, E. K. Hyde: Phys. Rev. C2, 1841 (1970)
3. K. Valli and E. K. Hyde: Phys. Rev. 176, 1377 (1968)
4. R. D. Macfarlane, R. A. Gough, N. S. Oakley, D. F. Torgerson: Nucl. Instr. Meth. 73, 285 (1969)
5. K. Valli, W. Treytl, E. K. Hyde: Phys. Rev. 161, 1284 (1967)
6. D. F. Torgerson and R. D. Macfarlane: Phys. Rev. C2, 2309 (1970)
7. R. S. Hager and E. C. Seltzer: Nucl. Data A4, 1 (1968)
8. J. S. Hansen, J. C. McGeorge, R. W. Fink, R. E. Wood, P. Venugopala Rao, J. M. Palms: Z. Phys. 249, 373 (1972)
9. C. M. Lederer: Program ICC, Lawrence Berkeley Lab report UCRL-19980, unpublished (1970)
10. I. Perlman and J. O. Rasmussen: Handbuch der Physik XLII p. 109 (Springer, Berlin 1957)
11. L. J. Jardine, S. G. Prussin, J. M. Hollander: Nucl. Phys. A190, 261 (1972)
12. K. H. Maier, J. R. Leigh, F. Pühlhofer, R. M. Diamond: J. Physique 32, C6-221 (1971)

13. M. R. Schmorak and R. L. Auble: Nucl. Data B5, 207 (1971)
14. L. J. Jardine: PhD thesis, Lawrence Berkeley Lab report LBL-246, unpublished (1971); L. J. Jardine, S. G. Prussin, J. M. Hollander: Lawrence Berkeley Lab Nucl. Chem. 1972 annual report LBL-1666, p. 9 (to be submitted to Nucl. Phys.)
15. T. Kempisty, A. Korman, T. Morek, L. K. Peker, Z. Haratym, S. Chojnacki: Joint Inst. for Nucl. Research report P6-6723 (DUBna, 1972)
16. D. G. Raich: PhD thesis, Yale University, unpublished (1976)
17. A. H. Wapstra, G. J. Nijgh, R. van Lieshout: Nuclear Spectroscopy Tables (North-Holland, Amsterdam, 1959); J. M. Blatt and V. F. Weisskopf: Theoretical Nuclear Physics, chapter VII.6 (Wiley, New York, 1952)
18. O. Nathan and S. G. Nilsson: Chapter X in Alpha-, Beta- and Gamma-ray Spectroscopy, ed. K. Siegbahn (North-Holland, Amsterdam, 1965)
19. J. O. Rasmussen, D. G. Raich, H. J. Mang, T. Fliessbach, L. Marquez. (to be submitted to Z. Phys.)
20. T. Fliessbach: Z. Phys. A272, 39 (1975)

Table 1. Gamma and x-ray activity of  $^{213m}\text{Ra}$

$$(T_{1/2} = 2.1 \pm 0.1 \text{ ms}).$$

The three main  $\gamma$ -rays are observed in nanosecond coincidence with one another and with the Ra  $K_{\alpha}$  x-rays.

(Parenthetical values are errors in the last digit reported.)

Transition energy (keV)	Relative photon intensity ( $I_{1063}=1.00$ )	Assigned multi-polarity	Relative transition intensity <sup>a)</sup>	K-vacancies due to transition
160.87(5)	0.46(2)	E2	1.08(4)	0.1108(40)
546.35(5)	1.04(3)	E2	1.08(3)	0.0223(6)
1062.5(2)	1.00(3)	E2	1.01(3)	0.0063(2)
			$\Sigma_{K\text{-vac}} = 0.139(4)$	
$K_{\alpha 1}$ 85.4	0.042(3)			
$K_{\alpha 2}$ 88.5	0.062(4)		0.137(6)	
$K_{\beta 1}$ 100.	0.021(3)			
$K_{\beta 2}$ 103.0	0.007(2)			

Millisecond component of  $\gamma$ -rays in  $^{209}\text{Rn}$

104.6(2)	0.0012(10)	E2(+M1)	0.009(8) [0.016(13)]
110.1(1)	0.005(2)	E2	0.032(8)
214.7(2)	0.010(3)	E2(+M1)	0.014(4) [0.026(8)]

Minute component of  $\gamma$ -rays in  $^{209}\text{Rn}$

104.6(2)	0.0042(15)	E2(+M1)	0.033(10)[0.05(2)]
110.1(1)	0.08(2)	E2	0.50(13)
214.7(2)	0.012(3)	E2(+M1)	0.017(4)[0.030(8)]

<sup>a)</sup> Calculated on basis of theoretical conversion coefficients from Hager and Seltzer[7] as listed in Table 2. X-ray transition intensities based on fluorescence yield  $\omega_K = 0.97$ , interpolated from values in ref.[8].

Table 2. Theoretical internal conversion coefficients for  $^{213m}\text{Ra}$  decay, calculated by computer interpolation[9] from tables of Hager and Seltzer[7]. (Parenthetical values indicate power of 10 by which to multiply preceding number.)

Element	Transition Energy (keV)	Multipolarity				
		E1	E2	E3	M1	M2
<u>Values of <math>\alpha_K</math></u>						
$^{88}\text{Ra}$	10.	----- less than K-binding energy -----				
	160.87	0.122	0.241	0.466	3.42	14.7
	546.35	8.10(-3)	0.0215	0.0532	0.120	0.301
	1062.5	2.37(-3)	6.30(-3)	0.0137	0.0210	0.0472
$^{86}\text{Rn}$	105	0.329	0.353	0.183	9.74	55.9
	110	0.293	0.368	0.283	8.50	47.5
	215	0.0593	0.145	0.361	1.29	4.95
<u>Values of <math>\alpha_{\text{total}}</math> (all shells)</u>						
$^{88}\text{Ra}$	10.	13.1	1.93(+5)	9.93(+7)	698.	6.28(+5)
	160.87	0.154	1.34	19.2	4.25	22.1
	546.35	9.90(-3)	0.0315	0.106	0.148	0.392
	1062.5	2.87(-3)	8.07(-3)	0.0191	0.0258	0.0596
$^{86}\text{Rn}$	105	0.420	6.84	168.	12.1	90.8
	110	0.374	5.59	129.	10.5	76.2
	215	0.0737	0.417	3.90	1.60	6.97

00004504659

Table 3. Gamma and x-ray intensities in coincidence spectra, and derived K-conversion coefficients. Intensities have been normalized as in table 1. (Parenthetical values are errors in the last digit reported.)

$E_{\gamma}$ (keV)	Gate (KeV)			$\alpha_K$	Closest assignment (Table 2)
	161	546	1063		
Ra K x-rays	0.024(8)	0.112(8)	0.135(9)	-	-
161	-	0.46(3)	0.45(3)	0.25(2)	E2
546	1.02(5)	-	1.04(5)	0.02(1)	(E2)
1063	1.00(5)	1.00(5)	-	0.005(10)	(E2)

Table 4. Results of Alpha Spectroscopy. (Parenthetical values are errors in the last digit reported.)

Isotope [ $Q_\alpha$ (MeV) <sup>a)</sup> ]	Present Work		Reported in Literature		
	$E_\alpha$ (MeV)	Decay %	$E_\alpha$ (MeV)	Decay %	Ref.
$^{213}\text{Ra}$ [6.893(5)]	6.731(5)	46(3)	6.730(5)	45(2)	[5]
	6.624(5)	47(3)	6.623(5)	49(2)	
	6.522(5)	6(1)	6.520(5)	6(1)	
	6.411(5)	0.5(1)	6.408	0.4	
$^{213m}\text{Ra}$ [8.663(5)]	8.467(5)	69(7)			
	8.358(10)	28(6)			
	8.266(10)	3(2)			
$^{214}\text{Fr}$			8.426(5)	93.0	[6]
			8.358(5)	4.7	
$^{214m}\text{Fr}$			8.549(8)	51(2)	[3]
			8.477(8)	49(2)	

Note: Ratio measured of  $\frac{^{213m}\text{Ra}}{^{213}\text{Ra}}$   $\alpha$ -decays =  $8.8(9) \times 10^{-4}$

(not corrected for cell's fast delivery fraction).

a) Corrected for recoil and screening, see ref.[10].

Table 5. Energies (keV) of  $\pi(h_{9/2}^n)_{J \neq 0}$  states in 126-neutron isotones

$J^\pi$	$^{210}_{84}\text{Po}$ n=2	$T_{1/2}$	$^{212}_{86}\text{Rn}$ n=4	$T_{1/2}$	$^{214}_{88}\text{Ra}$ n=6	$T_{1/2}$
2+	1181.4		1273.5		1381.2	
4+	1426.7	1.8 ns	1501.1		1637.1	32 ns
6+	1473.3	38 ns	1639.2	165 ns	1816.5	
8+	1556.8	110 ns	<1700	1.0 $\mu\text{s}$	1864	67 $\mu\text{s}$
Ref.	[11]		[12]		[12]	

## Figure Captions

[XBL 761-100]

Fig. 1. Schematic diagram of the helium-jet apparatus.

[XBL 761-99]

Fig. 2. Time distribution curve of 1.7-ms  $^{215}\text{Ra}$  activity delivered by helium-jet system.

[XBL 761-29]

Fig. 3. Gamma-ray spectra of 2.1-ms  $^{213\text{m}}\text{Ra}$  from two successive several-millisecond intervals immediately following irradiation. The beam lost about 5 MeV in the thin ( $\approx 10 \text{ mg/cm}^2$ ) target, for an average energy of roughly 81 MeV.

[XBL 739-4119]

Fig. 4. Excitation functions for some  $\gamma$ -rays observed following the bombardment of  $^{209}\text{Bi}$  by  $^{10}\text{B}$ . Vertical positioning of the curves is arbitrary and does not reflect the relative  $\gamma$ -ray intensities.

[XBL 761-41]

Fig. 5. Alpha-particle spectrum showing  $^{213\text{m}}\text{Ra}$ .

[XBL 761-40]

Fig. 6. Detail of two time intervals contributing to the  $\alpha$ -spectrum of Fig. 5.



Captions (Continued)

[XBL 761-145]

Fig. 7. Proposed  $^{213\text{m}}\text{Ra}$  decay scheme. Relative photon intensities (and uncertainties) are shown in front of transition energies. Approximate hindrance factors follow  $\alpha$ -feeding percentages.

[XBL 739-4120]

Fig. 8. Level trends and primary  $\alpha$ -cascades in 125-neutron isotones below  $^{213}\text{Ra}$ . See for  $^{207}\text{Pb}$  [13],  $^{209}\text{Po}$  [14], and  $^{211}\text{Rn}$  [3,6,15,16].

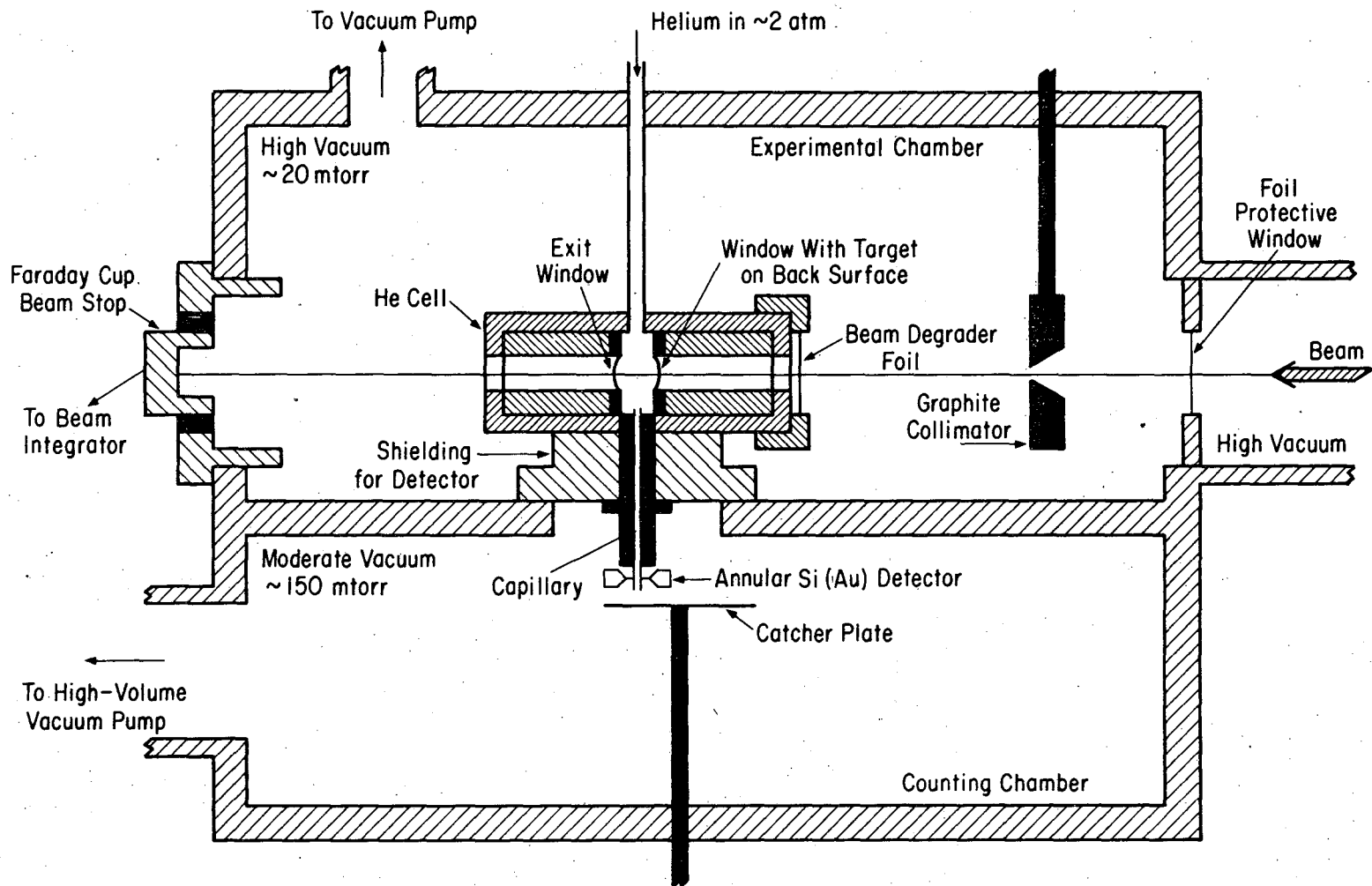
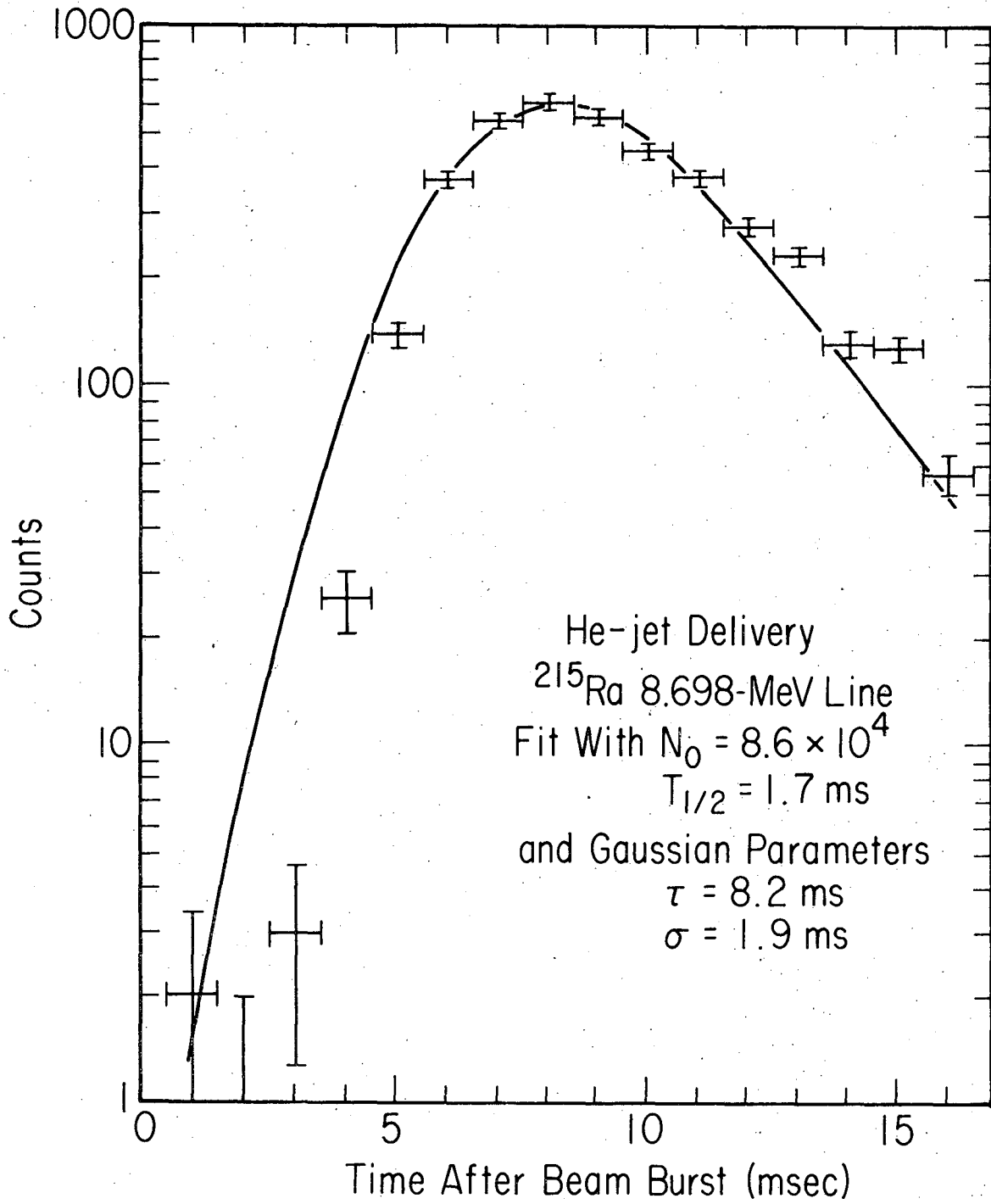


Fig. 1

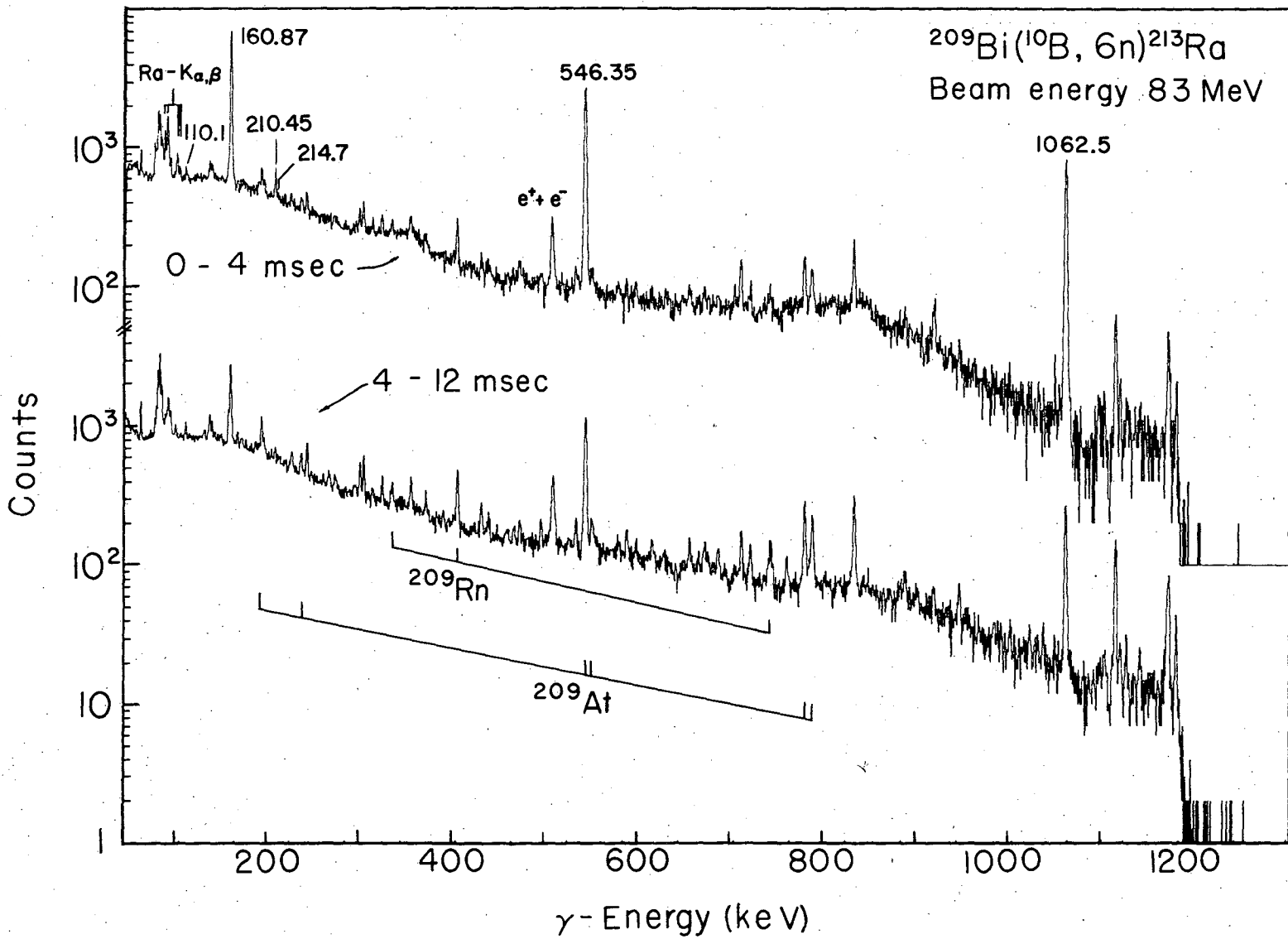
XBL 761-100

00004504661



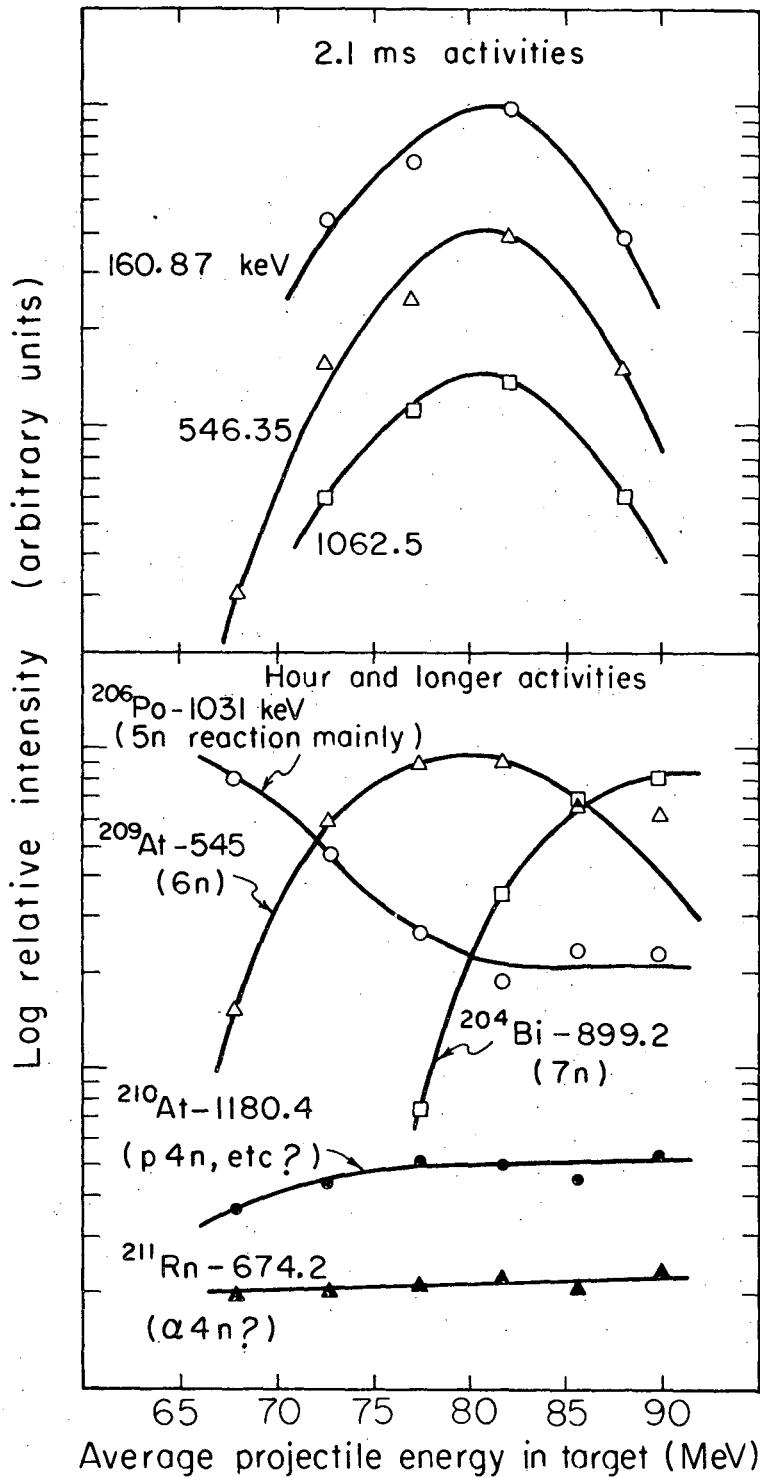
XBL 761-99

Fig. 2



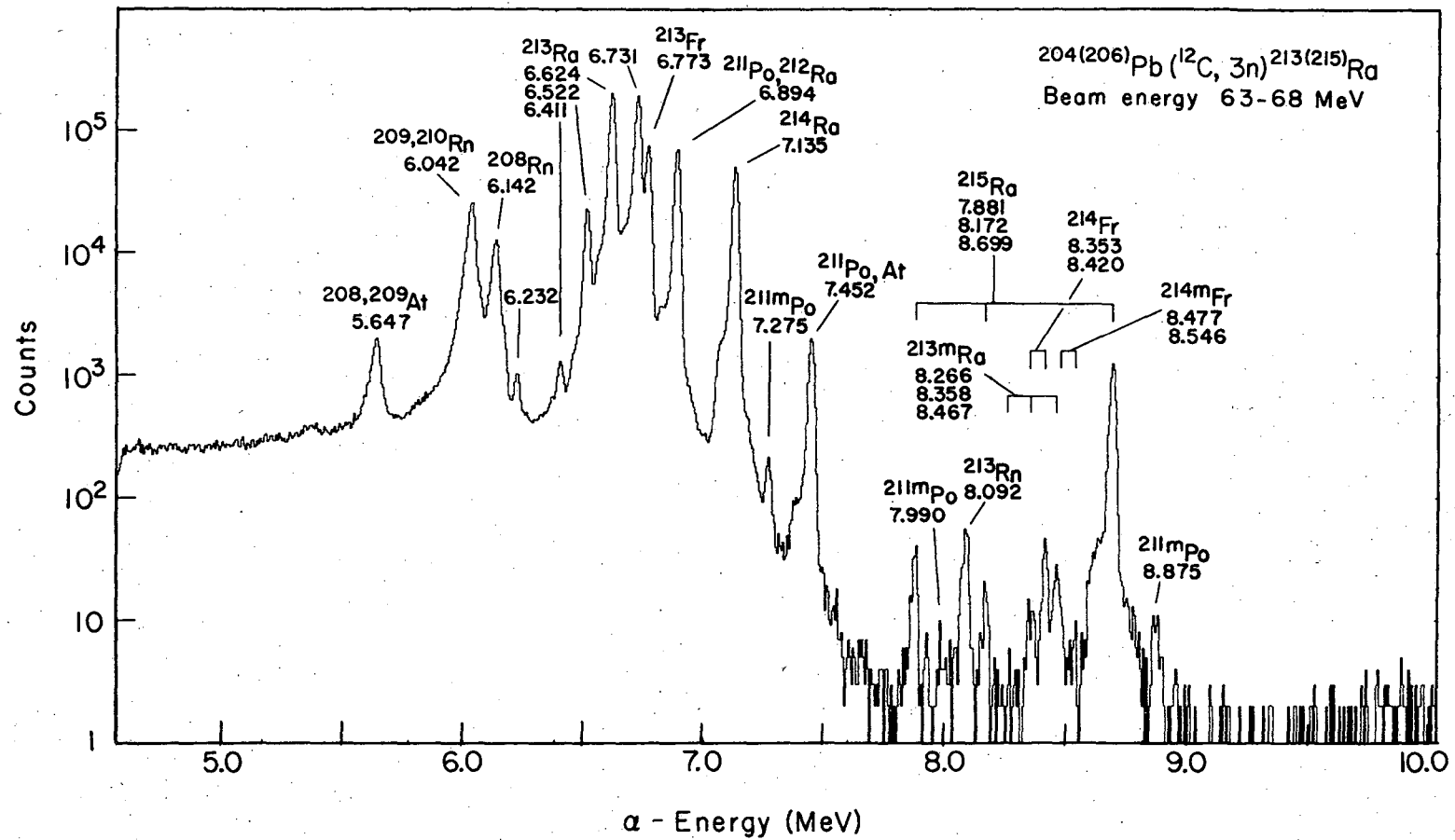
00004504662

Fig. 3



XBL739-4119

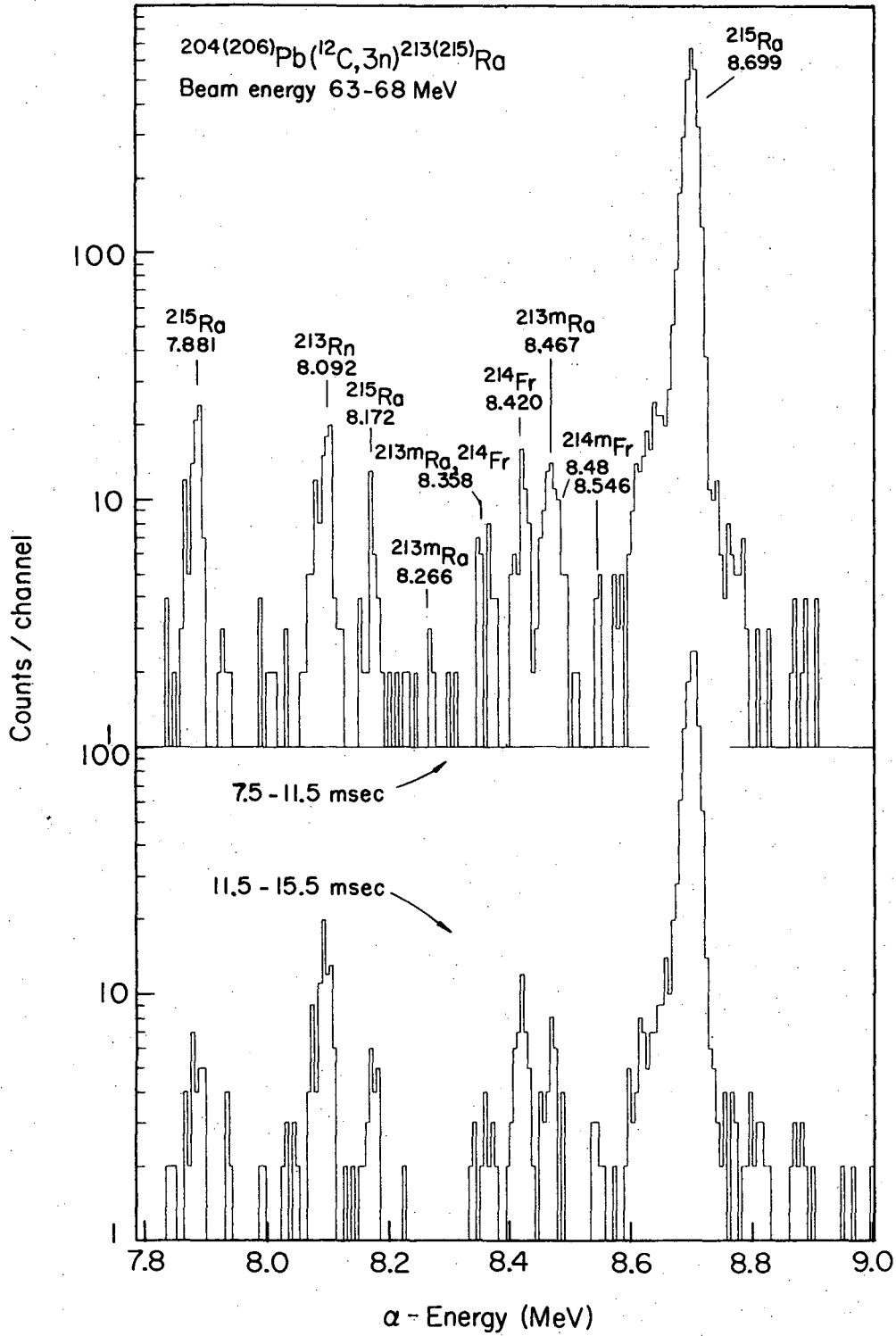
Fig. 4



00004504663

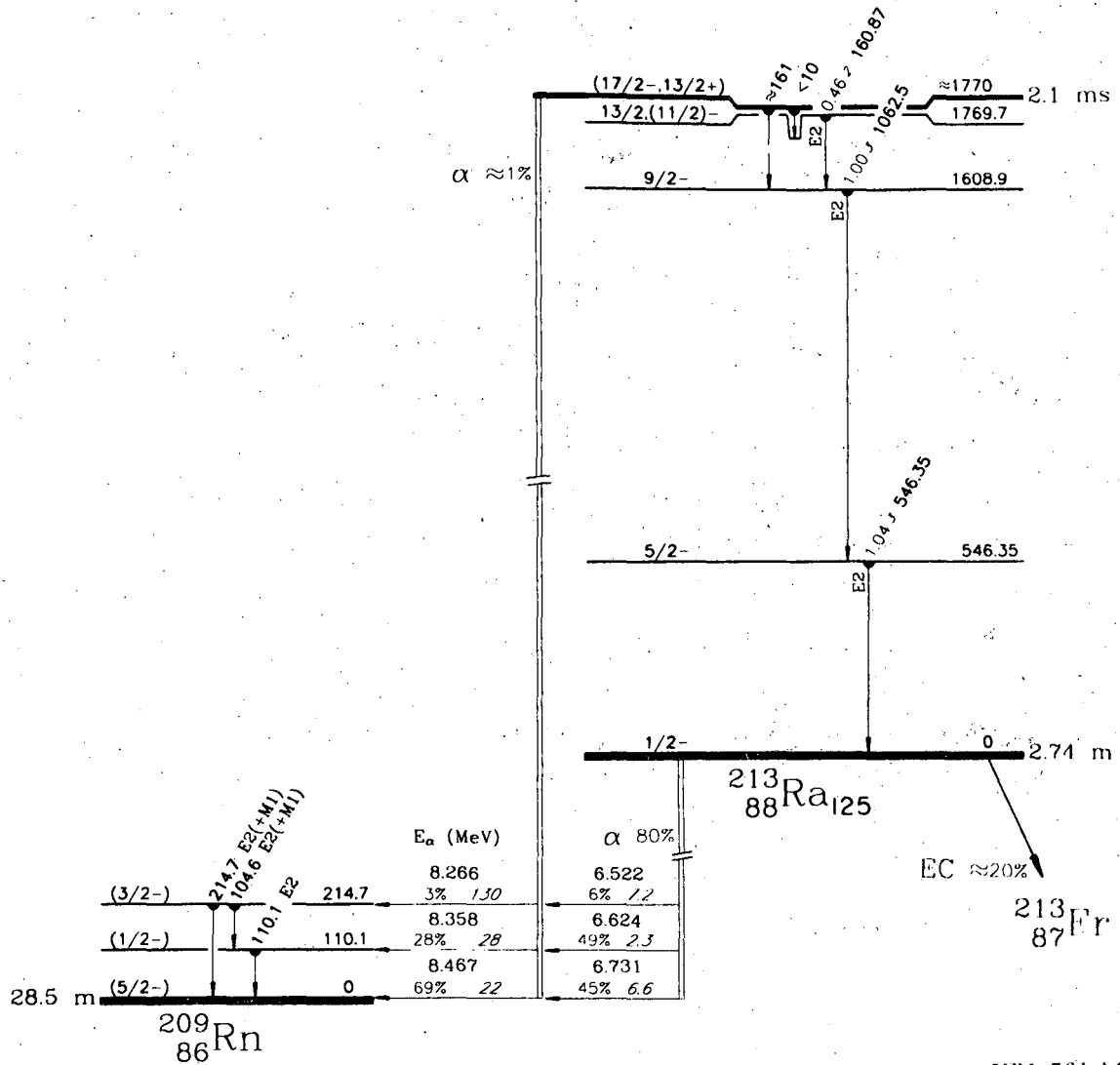
Fig. 5

XBL 761-41



XBL 761-40

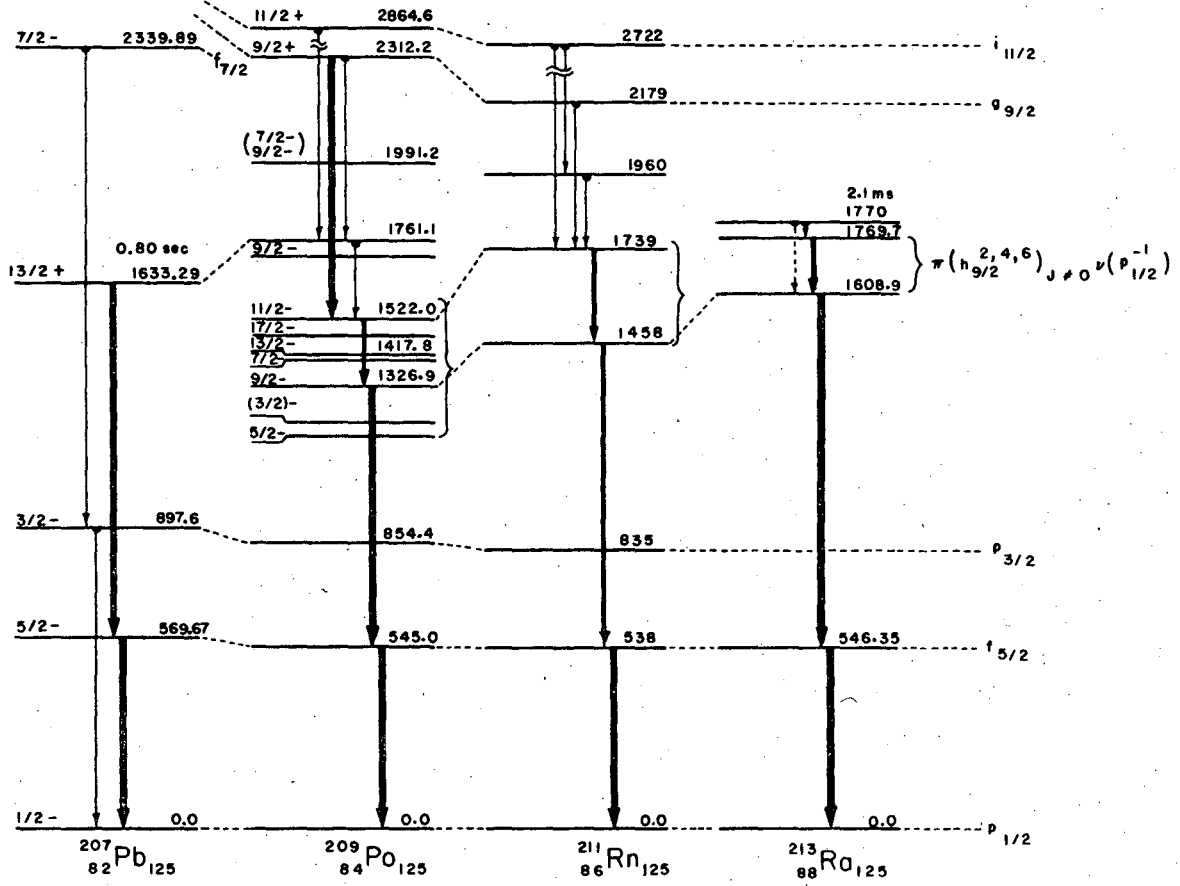
Fig. 6



XBL 761-145

Fig. 7





XBL739-4120

Fig. 8

**LEGAL NOTICE**

*This report was prepared as an account of work sponsored by the United States Government. Neither the United States nor the United States Energy Research and Development Administration, nor any of their employees, nor any of their contractors, subcontractors, or their employees, makes any warranty, express or implied, or assumes any legal liability or responsibility for the accuracy, completeness or usefulness of any information, apparatus, product or process disclosed, or represents that its use would not infringe privately owned rights.*

TECHNICAL INFORMATION DIVISION  
LAWRENCE BERKELEY LABORATORY  
UNIVERSITY OF CALIFORNIA  
BERKELEY, CALIFORNIA 94720